Assessment of methods used in 1D models for computing bedload transport in a large river: the Danube River in Slovakia

B. Camenen, K. Holubova, M. Lukac, J. Le Coz, André Paquier

▶ To cite this version:

Assessment of methods used in 1D models for computing bedload transport in a large river: the Danube River in Slovakia

B. Camenen [a,*], K. Holubová [b], M. Lukač [b], J. Le Coz [a], and A. Paquier [a]

[a] *Cemagref, UR HHLY, 3 bis quai Chauveau, CP 220, F-69336 Lyon cedex 09, France*

[b] *Water Research Institute (WRI-VUVH), Bratislava, Slovakia*

Abstract

Comprehensive measurements of bedload sediment transport through a section of the Danube River, located approximately 70km downstream from Bratislava, Slovakia, are used to assess the accuracy of bedload formulae implemented in 1D modelling. Depending on water discharge and water level, significant variations in the distribution of bedload across the section were observed. It appeared that, whatever the water discharge, the bed shear stress τ is always close to the estimated critical bed shear stress for the initiation of sediment transport τ_{cr}. The discussion focusses on the methods used in 1D models for estimating bedload transport. Though usually done, the evaluation of bedload transport using the mean cross-sectional bed shear stress yields unsatisfactory results. It is necessary to use an additional model to distribute the bed shear stress across the section and calculate bedload locally. Bedload predictors also need to be accurate for τ close to τ_{cr}. From that point of view, bedload formulae based on an exponential decrease of bedload transport close to τ_{cr} appear to be more appropriate than models based on excess bed shear stress. A discussion on the bedload formula capability to reproduce grain sorting is also provided.

Key words: bedload; measurements; 1D model; bed shear stress distribution; bedload distribution; Danube

* Corresponding author.
 Email address: `benoit.camenen@cemagref.fr` (B. Camenen).

1 Introduction

Because of the increasing importance of research and management problems in water development and environmental protection, knowledge of the reliability of the sediment transport measurements and predictors are of great importance. As for many large rivers, the bed dynamics in the Danube River changed dramatically after the construction of continuous flood protection lines (Holubová *et al.*, 2004). The navigation channel created at the end of XIXth century needs permanent dredging in order to keep proper navigation conditions. Moreover, as a result of the construction of water structures in the Austrian river reach in the second half of the XXth century, a decrease in sediment transport by 80% was observed in Slovakia. Extensive commercial dredging initiated erosion of the river bed downstream from Bratislava. As a result an erosion of the river bed occurred downstream from Bratislava, resulting in an increase in the differences between river bed and meander levels, and so, in a reduction of the meander dynamics and sediment input in the Danube River. Despite the Autrian development of stategies for improvement and management of the Slovak-Austrian Danube (Holubová *et al.*, 2004), bedload transport is not stabilized with tendencies of aggradation upstream of Bratislava. Since the construction of the Gabčikovo dam in 1992, an approximate 5m-deep erosion feature on the Danube river bed is now propagating downstream and needs to be better understood.

Empirical functions have been developed for predicting mean sediment transport from river discharge or stream power (Leopold & Emmett, 1976). However, such functions are site-specific and need careful calibration to be applicable. As sediment transport measurements and especially bedload measurements are generally lacking, methods to estimate sediment transport rates need to be improved to reduce as much as possible the uncertainties of the prediction. More recently, 1D hydraulic models have been used to estimate sediment transport capacity (Thomas & Prashum, 1977 among others). These models allow the computation of the mean velocity and mean bed shear stress averaged over a cross-section of the river. The estimation of the sediment transport rate is then often calculated by applying classical sediment transport formulations such as the Meyer-Peter & Müller (1948) or Ackers & White (1973) formulae using the computed mean bed shear stress or/and mean velocity. Consequently, many field studies focussed on the total bedload transport throughout a section (Bunte et al., 2004 among others), even for large river cross-sections (Nile: Gaweesh & Van Rijn, 1994, Abdel-Fattah et al., 2004; Frazer River: Mc Lean et al., 2009). Kleinhans & Ten Brinke discussed the

accuracy of the measurements for a large river section, with however, no physical support for the bed shear stress and bedload distribution. Habersack & Laronne (2002) made an extensive evaluation of classical bedload formulae compared to field measurements on the Drau River using section averaged hydraulic parameters. The performance of the formulae appeared to be very poor for low bed shear stress and often overestimated for larger bed shear stress. They also observed that the application of local hydraulic parameters improves the results. Habersack et al. (2008) showed a significant variability in the cross-sectional distribution of bedload and concluded that a 2D description is necessary. To the authors knowledge, there are few studies on the modelling and measurement of the distribution of the bedload transport throughout a large river section. Seed (1996) made an interesting numerical study on lateral variation of sediment transport in rivers. He used the method of Shiono & Knight (1991) for the velocity distribution across the section and showed significantly different results by applying bedload formulae on section-averaged parameters or laterally varying parameters. The section-averaged method yields large underpredictions when the mean bed shear stress is close to its critical value for inception of transport; it yields overpredictions for large bed shear stresses when river section is irregular.

The purpose of this paper is to assess how accurately the bedload transport formulae (calibrated for local sediment transport) used in 1D modelling can predict the observed rates on a large river. The present paper does not use any numerical 1D model but experimental data to validate the suggested improvement of methods for computing bedload transport to be applied in a 1D model. Using field measurements conducted in a large section of the Danube River, a discussion is provided on the distribution of the bed shear stress and bedload transport throughout a river section and its importance on the prediction of the total bedload. For such rivers where bed shear stresses are relatively low, it appears also fundamental to use a formula that accurately predicts bedload transport for bed shear stresses close to the critical value for incipient motion. For that purpose, the results obtained using two similar formulae (Meyer-Peter & Müller, 1948, and Camenen & Larson, 2005), which differs only in the way they handle critical bed shear stress are compared. The effect of the grain size on the results is presented for both studied formulae. A discussion on the model capability to reproduce grain sorting is also provided.

3

2 Bedload measurements

In order to study the impact of hydropower schemes on the river morpho-dynamic processes, bedload measurements were carried out in the Slovak-Hungarian Danube during the research programme *Changes in sediment transport regime of the Danube River, downstream of Gabčikovo HPP (1999-2002)* (Holubová *et al.*, 2004).

2.1 Site location

Bedload measurements were conducted downstream of the hydropower plant built in 1992 at Gabčikovo (km 1795.58, *cf.* Fig. 1) approximately 15km downstream the confluence between the Old Danube and the navigation canal. A few kilometres downstream (km 1788, next to Kližska Nemá village), a significant change of the bed slope is observed: the Danube River changes from a submontane river (with a bed slope $i \approx 0.3\%$) to a lowland river ($i \approx 0.04\%$). The reference discharges were estimated from the gauging station at Medvedov (km 1806.40, next to the Medvedov bridge).
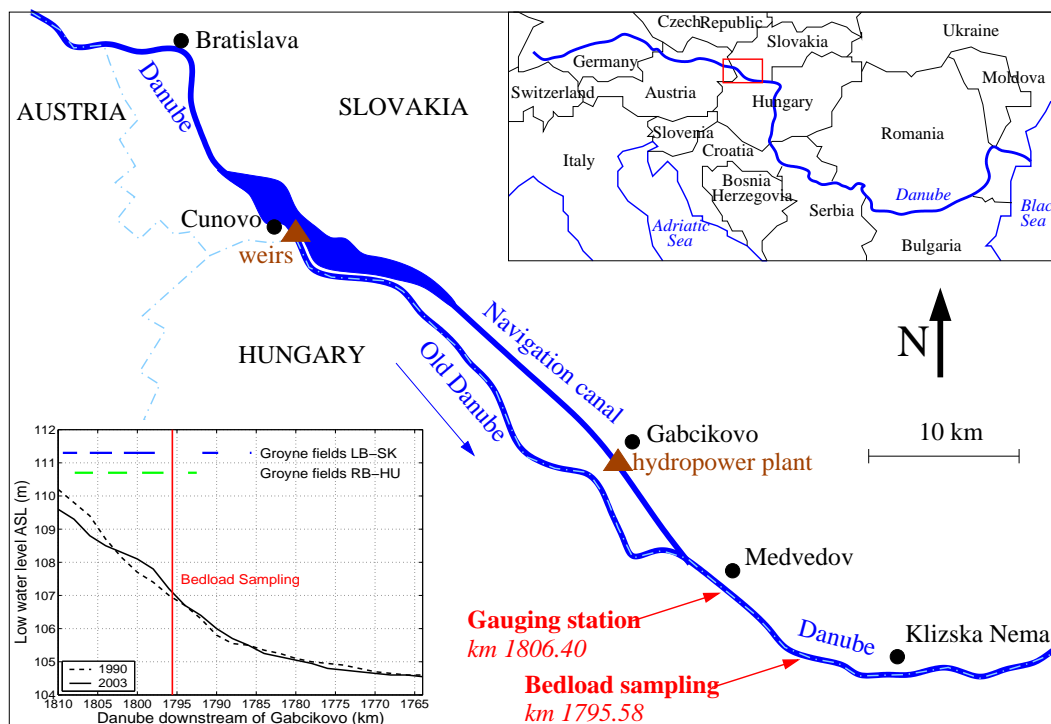

Fig. 1. Location of the field measurements on the Danube River; low water levels in 1990 and 2004 and position of the groyne fields (bottom left insert).

With regard to some evidences of bedform existence in the Danube river bed, two sets of five longitudinal profiles were recorded by echosounder (7 km long river section) to provide information about the river bed topography and to select the bedload measurement location. Results indicated areas with flat bed, transitional zones and some areas where gravel dunes are developed. Height of dunes ranges from 0.4 m to 0.8 m and the length varies between 7m - 20 m. Subsequently an area with flat bed was chosen to provide optimal conditions for bedload measurements (proper position of bedload sampler on the river bed) and minimize the effect of dune formation on flow characteristics and bedload transport. In the same idea, the location was chosen to avoid direct influence of groyne fields on the local flow (see bottom left insert of Fig. 1). However, it should be noted that groyne fields located upstream of the bedload sampling may influence the local water slope depending on the discharge.

2.2   Method of field data collection

Bedload measurements were collected using a basket-type bedload sampler similar to the Ehrenberger (1931) model modified by VUVH (WRI), with a mesh size of 3 mm and a trapping efficiency of 0.7 (*cf.* Fig. 2a and b). Between 2000 and 2002, bedload transport measurements were undertaken throughout one cross-section during 71 campaigns for discharges varying from $972 \, \mathrm{m}^3 \, \mathrm{s}^{-1}$ to $4745 \, \mathrm{m}^3 \, \mathrm{s}^{-1}$. For each campaign, bedload samples were weighted and sieved at six verticals across the section. In order to minimize the error due to temporal fluctuations in bedload rate, each measurement (lasting from 2 to 5 min depending on the bedload transport intensity) was repeated 10 times to derive an averaged value for each vertical. Simultaneously, measurements of the vertical velocity profile were carried out at each vertical using a torpedo current-meter (*cf.* Fig. 2c). Velocities were measured at 5 elevations: near the free-surface, near the bottom, and at relative depths 0.8, 0.6, 0.2 from the free-surface following the ISO748 standard (2007). Water level fluctuations during the time of the experimentation were also recorded.

During the bedload sampling programme, the cross-section bathymetry was surveyed on four occasions (Fig. 3a). Systematic deposition occurred in the central part of the river channel ($\Delta z \approx +1.5$ m) whereas a slight erosion ($\Delta z \approx -0.5$ m) occurred on the left side of the river section. Bedload samples taken across the section (Fig. 3b) indicate nearly constant grain size distributions across the section: on average, the median grain size is $d_{50} = 9$ mm and the grain diameter exceeded by 10% and 90% by weight of sample are $d_{90} = 18$ mm, and $d_{10} = 5$ mm, respectively. Bed material was also sampled at six

Fig. 2. Field measurements across the Danube section at km 1795.58: a) Basket–
type bedload sampler (modified by VUVH); b) Bedload material collected from the
sampler; c) Suspended-load sampler and torpedo current meter.

verticals at the same location (*i.e.* km 1795.58). It appears that bed material
is very similar to the bedload material: The bed material median grain size
$d_{b,50}$ is the same as the bedload material median grain size: $d_{b,50} = 9$ mm.
The bed grain diameter exceeded by 10% and 90% by weight of sample are
$d_{b,90} = 22$ mm, and $d_{b,10} = 3$ mm, respectively. The difference in grain size,
$d_{b,90} > d_{90}$, indicates that coarser sediments are only partially transported.
$d_{b,10} < d_{10}$ may be explained by the mesh size of the bedload sampler, which
is 3 mm. Therefore, the bedload grain size analysis is slightly biased since fine
sediment content is underestimated.

Discharges were estimated for each period of bedload sampling based on the
hydrometric gauging station located 11.82 km upstream (km 1806.40) from
the measurement location (*cf.* Fig. 1). Fluctuation of water levels during the
measurements were recorded at three temporary gauging stations (one was
located at the section of bedload measurements, the other two 1km upstream
and downstream of the first one, respectively).

3 Local bedload predictions

Most of the equations that have been developed to estimate the bedload trans-
port rate were calibrated with local sediment transport measurements (at the
centre of a uniform flow). First, field data from the Danube River were used to
evaluate the predicting capability of selected formulae for local bedload trans-
port. Assuming a logarithmic vertical velocity profile, the bed shear stress was
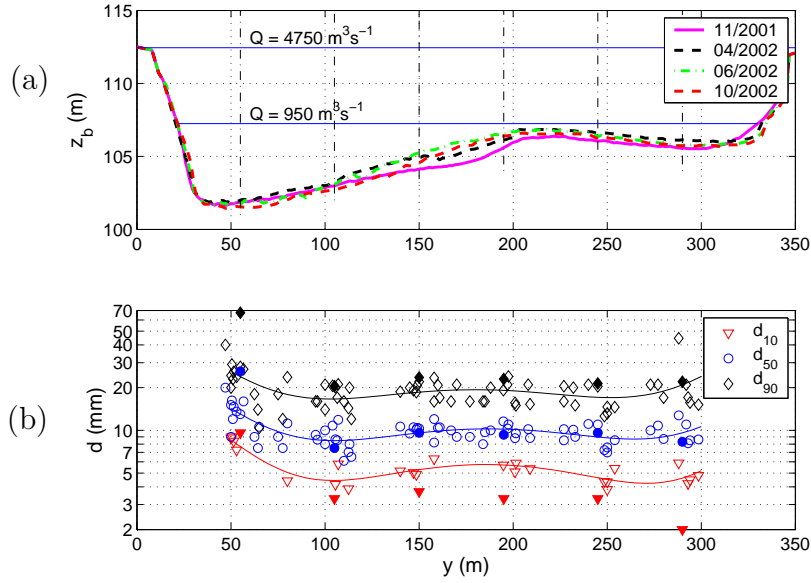
Fig. 3. Bottom evolution of the cross-section where bedload measurements were carried out (a) and grain size characteristics of the bed (solid symbols) and bedload (open symbols) samples across the section (b).

estimated using a fit of velocity measurements taken from several points in a vertical. Current velocities were measured at 5 elevations $z/h = 0.05, 0.2, 0.4, 0.8,$ and 0.95, where z is the height above the bed and h the local water depth. An additional point was estimated for the zero velocity assumed at $z_0 = k_s/30$, where k_s is the roughness height. As previously observed by Kamphuis (1974) and Yalin (1977), Camenen et $al.$ (2006) observed a relative roughness ratio scattered around a constant value of $k_s/d_{90} = 2$ for flat beds with low sediment transport. Accordingly, the roughness height was set to $k_s = 2d_{b,90}$ (d_{90} estimated from the bed material characteristics). This zero-velocity point was added because large dispersion on the bed shear stress was observed using the 5 point-velocity measurements only. It should also be noted that bed shear stress should normally be derived from the lowest 20% part of the velocity profile (Graf, 1971). However, several authors (Cardoso et al., 1989, Sumer et al., 1996, or Smart et al., 2002) observed that the log-profile may be valid for $z/h < 0.6$. The mean value as well as the standard deviation of the ratio $R = z_{0,est}/z_0$ was calculated with or without the additional point, where $z_{0,est}$ is the estimated roughness length from the logarithmic fit and $z_0 = 2d_{b,90}/30$: $(\bar{R}, \mathrm{std}(R)) = (1.2, 0.3)$ for the first case whereas $(\bar{R}, \mathrm{std}(R)) = (5.9, 13.4)$ for the second case. Then, the Shields parameter θ was computed using the logarithmic law for computing the friction coefficient f_c, $i.e.$:

$$\theta = \frac{\tau}{(\rho_s - \rho)gd_{b,50}} = \frac{1/2 \, f_c U^2}{(s-1)gd_{b,50}} \tag{1}$$

with
$$f_c = 2 \left(\frac{\kappa}{1 + \ln(z_{0,est}/h)} \right)^2 \tag{2}$$

where τ is the bed shear stress, U is the mean velocity over the local water depth h, $d_{b,50}$ is the bed material median grain size, $\kappa = 0.41$ is the von Karman constant, $s = \rho_s/\rho = 2.65$ is the relative density of the sediment, and ρ_s and ρ are the density of the sediment and water, respectively. Since $k_{s,est} = z_{0,est}/30 \approx k_s$, the estimated bed shear stress τ corresponds to the grain related bed shear stress, and so, does not take into account a possible form drag. It should correspond to the effective bed shear stress that is acting on the bed.

Bedload sediment transport rates q_s (in $\mathrm{m^3 \, s^{-1} \, m^{-1}}$) at each location measured on the Danube were plotted against the local Shields parameter θ (cf. Fig. 4). The scatter in the experimental results gives an indication of the difficulties in the estimation of the bedload transport. First, there are some uncertainties in the estimation of bedload using a bedload sampler due to the experimental apparatus but also due to the bedload fluctuations and variabilities, especially for a non-uniform mixture. Second, there are also significant uncertainties in the estimation of the bed shear stress using 5 point-velocity measurements, which were not sufficient for a more detailed analysis. Moreover, the method used here for estimating the bed shear stress tends to reduce its value to the grain-related bed shear stress. Bedforms may also influence both bed shear stress and bedload transport measurements. However, no bedform was observed and current ripples seldom occur for such coarse sediments (Allen, 1985). Another interesting point is that measured bed shear stresses appeared to be always relatively low $(\max(\theta) < 0.1)$ and close to the critical value for inception of transport whatever the water discharge observed on the Danube at this location.

For this reason, we choose to compare two similar bedload formulae, which are both based on the shear stress concept and differ only in the representation of the critical bed shear stress effects on bedload transport, i.e. excess bed shear stress versus exponential decrease of bedload transport close to τ_{cr}. The first formula is an extension of the the Meyer-Peter & Müller (1948, noted hereafter MPMe) equation including a critical Shields parameter, which may differ from the value suggested by Meyer-Peter & Müller $(\theta_{cr} = 0.047)$ based on their own data set. The second formula is the Camenen & Larson (2005, noted hereafter CL) equation, which is a modification of the MPMe model
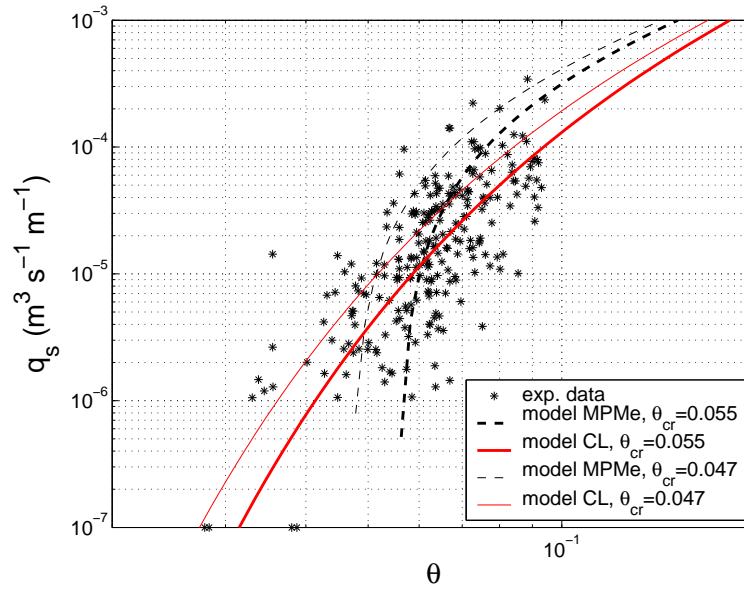
8

Fig. 4. Local bedload transport as a function of the local Shields parameter (MPMe: Meyer-Peter & Müller type formula, CL: Camenen & Larson formula).

based on a probabilistic approach for the inception of bedload transport as suggested by Einstein (1950). These formulae may be written as follows:

$$\text{MPMe :} \qquad \frac{q_s}{\sqrt{(s-1)gd_{50}^3}} = 8(\theta - \theta_{cr})^{3/2} \qquad (3)$$

$$\text{CL :} \qquad \frac{q_s}{\sqrt{(s-1)gd_{50}^3}} = 12\theta^{3/2} \exp\left(-4.5\frac{\theta}{\theta_{cr}}\right) \qquad (4)$$

where q_s is the local bedload transport expressed in $\text{m}^3 \text{ s}^{-1}\text{m}^{-1}$, d_{50} is the median bedload material size (It should be noted that bed shear stress has to be computed using bed characteristics whereas bedload rate has to be made dimensionless using bedload characteristics), and θ_{cr} is the critical Shields parameter for the inception of sediment transport. Shields (1936) showed that θ_{cr} is a function of the grain size. Using the Soulsby (1997, p.106) formula for the Shields curve as a function of $d_{b,50}$, $\theta_{cr} \approx 0.055$ was obtained for the present study case.

Both equations have been superimposed on the data in Fig. 4 using two different critical Shields parameter, $\theta_{cr} = 0.047$ as suggested by Meyer-Peter & Müller (1948) and $\theta_{cr} = 0.055$ as given by the Shields curve. Both MPMe and CL formulae are in relatively good agreement with the data with respect to the measurement uncertainty and the assumption of single grain size for the computation. For many cases, the computed Shields parameter is lower

9

than the estimated critical Shields parameter for the inception of sediment
transport, though sediment transport was observed. Taking into account un-
certainties in the estimation of the bed shear stress (a priori underestimated
as $k_s \geq 2d_{90}$ when bedload occurs, see Camenen et al., 2006; Recking et al.,
2008) or of the critical bed shear stress (a priori overestimated looking at the
experimental results), the CL formula appears to be more appropriate since
it yields non-zero bedload transport rates even if $\theta < \theta_{cr}$. Indeed, there are
large uncertainties in the estimation of the critical Shields parameter for a
sediment mixture but also in the definition of the critical Shields parameter
(first individual movement to full mobility of the surface layer, see Buffington
& Montgomery, 1997). Moreover, when $0.7 \leq \theta \leq 0.9$, the MPMe formula
tends to over-estimate the measured bedload rates while the CL formula is
more in agreement with field data (see also Camenen & Larson, 2005). If the
original MPM model is used (i.e. MPMe with $\theta_{cr} = 0.047$), results are slightly
improved for lower bed shear stress but the overestimation is even stronger
when $0.7 \leq \theta \leq 0.9$. $\theta_{cr} = 0.055$ will be used hereafter since the results are
slightly better for both formulae and it corresponds to the value given by the
Shields curve for the measured grain size.

4   Distribution of bedload across the section

4.1   Estimation of the section-averaged bed shear stress from experimental data

The section-averaged total bed shear stress τ_{mt} may be estimated using the
local slope S,

$$\tau_{mt} = \rho g R_h S \tag{5}$$

where R_h is the hydraulic radius. τ_{mt} includes energy loss from the interaction
between the main channel and the side walls and floodplain as well as from
possible bedforms (even if they were not observed). As observed in Fig. 5,
there is a large scatter in the estimation of the local slope S as a function
of the discharge. It gives an indication of the unsteadiness of the flow dur-
ing the experiments (achieved during floods). However, an interesting point is
the clear tendency of slope decrease with increasing discharges, which may be
explained by a larger energy dissipation due to the interaction with the flood-
plain. Using a 1D model, the effective bed shear stress for bedload transport
may be approximated using the empirical correction factor (Meyer-Peter &

Müller, 1948; see also the discussion by Wong & Parker, 2006),

$$\alpha_{cor} = \left(\frac{K_s}{K}\right)^{3/2} \tag{6}$$

where K and K_s (in m$^{1/3}$/s) are the total and grain-related Strickler coefficients, respectively ($\tau_{eff} = \alpha_{cor}\tau_{mt}$). For the grain-related Strickler coefficient, the formula $K_s = 23/k_s^{1/6} \approx 39\text{m}^{1/3}/\text{s}$ (Wong & Parker, 2006). The total Strickler coefficient was roughly estimated, $K = 35\text{m}^{1/3}/\text{s}$, in order to obtain similar results as from the velocity measurements (see Fig. 6b). However, this coefficient should vary with discharge as the influence of the side walls (including the floodplain) is getting higher. Thus, significant uncertainties exist in the computation of the effective bed shear stress estimated from the local slope measurements.
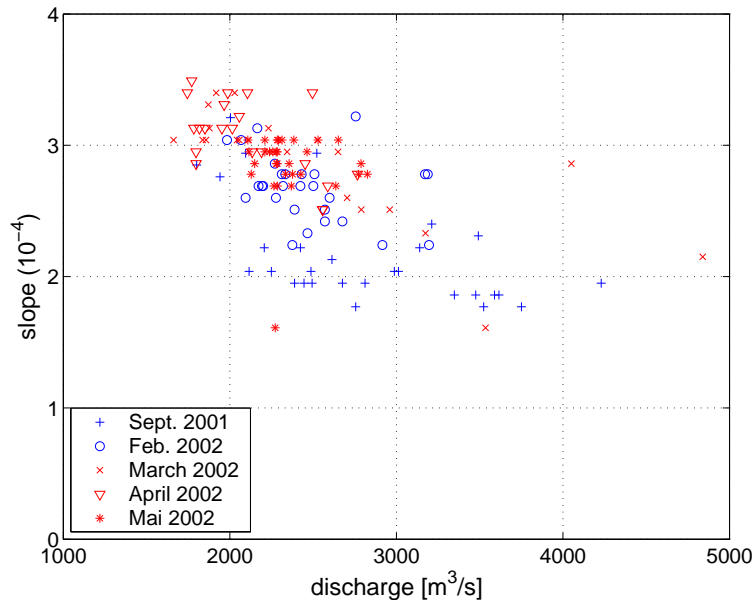

Fig. 5. Measured local water slope at the position of the bedload measurements versus water discharge.

Using a properly calibrated 1D model, it is possible to estimate the mean velocity over the section, $V_m(z_w) = Q(z_w)/A(z_w)$, where A is the wetted area, and z_w is the water level. Assuming a roughness height $k_s = 2d_{b,90}$ homogeneous throughout the section, the mean Shields parameter θ_m may be computed as a function of the water depth, *i.e.*

$$\theta_m = \frac{1/2\ f_c V_m{}^2}{(s-1)gd_{b,50}} \tag{7}$$

with $f_c = 2[\kappa/\{1 + \ln(z_0/R_h)\}]^2$, $z_0 = k_s/30$. It should be noted that θ_m corresponds here approximately to the effective Shields parameter.

11

The results that should be obtained using a 1D model have been estimated using a polynomial fit applied to the measured depth-averaged velocities. For discharges lower than $Q < 1000$ m^3 s^{-1} (no experimental data), a linear function of the discharge was assumed as a first estimate. It appears that V_m is an increasing function of the discharge Q when $Q < 2500$ m^3 s^{-1}, and is nearly constant ($V_m \approx 1.7$ m/s) when $Q > 2500$ m^3 s^{-1} (*cf.* Fig. 6a). This may be explained as for $2500 < Q < 5000$ m^3 s^{-1}, the bed roughness is getting small compared to the water depth, the bed level may be deeper, the influence of the side walls (including effects of the system of groynes located upstream) is getting higher, and an interaction with the floodplain is possible within the studied reach (see also Fig. 5). Because of the change in the bed slope downstream, some backwater effects may also appear for these large discharges. Measurements (velocity and local slope measurements) for high discharges ($Q > 3000$ m^3 s^{-1}) are too scarce to confirm this trend. The low value observed for $Q = 3750$ m^3 s^{-1} could also be explained by the limited number of verticals where the measurements were taken and the unsteadiness of the flow.

The calculated values of θ_m based on V_m are in good agreement with field data since the relation between V_m and θ_m is straightforward (*cf.* Fig. 6b). The nearly constant value for V_m when $Q > 3000$ m^3 s^{-1} yields a decreasing value of the Shields parameter with Q because the friction coefficient is decreasing with an increasing water depth (*cf.* Eq. 2 where k_s is assumed constant). The horizontal error bar corresponds to the range of water discharge data used to estimate the mean velocity and mean bed shear stress. The vertical error bar corresponds to the sum of a constant error in the velocity measurements ($E_{V,meas} = 0.1$ m s^{-1} based on the ISO748) and an error from the number of verticals n in the cross-section ($E_{V,nbr} \propto 1/\sqrt{n}$). If E_V and E_θ are the errors in the velocity measurement and Shields parameter estimation, respectively, one has $E_\theta = 2\theta/V\ E_V$. Additionally, it may be observed in Fig. 6(b) that results from the calculation of the effective bed shear stress based on local water slope measurements, although more scattered, are in good agreement with the previous observations.

4.2   Distribution of bed shear stress throughout the section

In order to estimate bedload transport throughout the cross-section, it is necessary to estimate the bed shear stress distribution. This implies an additional sub-model to the 1D model. Based on the merged perpendicular method (noted MP method hereafter, see Khodashenas & Paquier, 1999), the bed shear
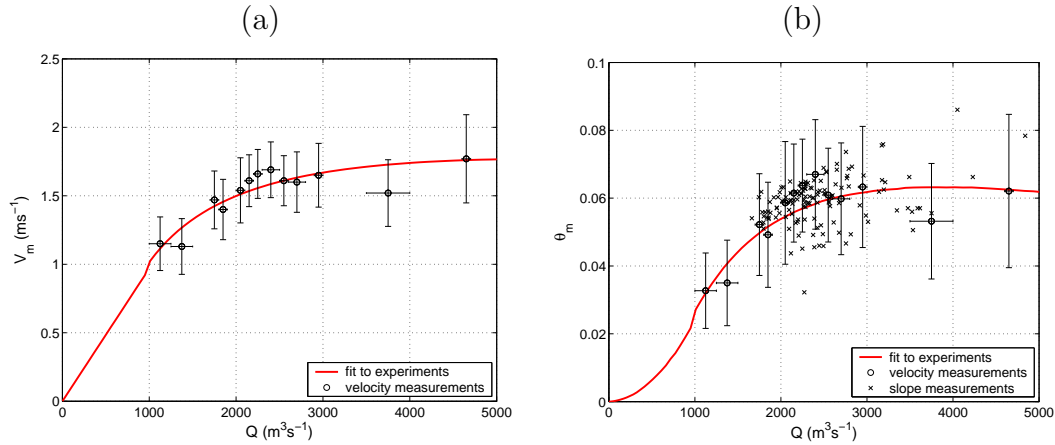
Fig. 6. Estimation of the variation of the mean velocity (a) and mean bed shear stress (b) with discharge.

stress is estimated across the section neglecting transverse bottom slope. Thus, the local hydraulic radius equals the vertical distance from the bottom to the first delimiter, which is either a bissector (geometrical division line between the flow influenced by the bank roughness and the flow influenced by the main channel roughness) or the water surface. Yang & Lim (1997) suggested that the direction of energy transportation is always along the minimum relative distance from the energy source to a boundary. Applying this concept to trapezoidal channels, the division lines between the bed and the walls are governed by $l_w/k_{sw} = l_b/k_{sb}$ where l_w and l_b are the normal distances from the division line to the side walls and bed, respectively, k_{sw} and k_{sb} are the side wall and bed roughness heights, respectively (Hey, 1979). The roughness on the banks (or side wall) includes effects of vegetation, longitudinal variation of the channel, etc. whereas the roughness of the river bed is linked to the bed material grain size, to the bedforms, or to the bedload intensity. Thus, the river bed roughness is generally much smaller than the bank roughness. Assuming a roughness on the banks X_b times larger than the main channel (bed) roughness, the bissectors are then defined using the angle α_b between the bed and the bissector and the angle α_w between the bank and the bissector, and the equation $\sin\alpha_w/\sin\alpha_b = X_b$. $X_b = 3$ was chosen in order to get the location of the maximum bed shear stress across the section correctly estimated (varying from the position of $y = 60$ to 90 m for Q=950 to 4750 m^3 s^{-1}).

Based on the method described above, the bed shear stress distribution was plotted for four typical values of the water discharge (Fig. 7b). These results are in good agreement with the data presented in Fig. 7a where field data are gathered for several ranges of water discharge surrounding the four chosen values. Polynomial fits for each set of data points corresponding to these ranges

of water discharge are also plotted in Fig. 7a. However, topography effects seem
to be overestimated, especially for the large values of the water depth. Indeed,
the model yields bed shear stress variations of a factor 2 between the left and
the right side of the river whereas measurements indicate a lower difference
(factor 1.5). These results could be improved using a more complex model
for the bed shear stress distribution including secondary currents such as the
model by Shiono & Knight (1991). It is also very important to realize that
the Shields parameter is always lower than 0.1 and very often lower than its
estimated critical value for inception of movement ($\theta_{cr} = 0.055$). In a large
river like the Danube River, bed shear stresses appear to be often close to the
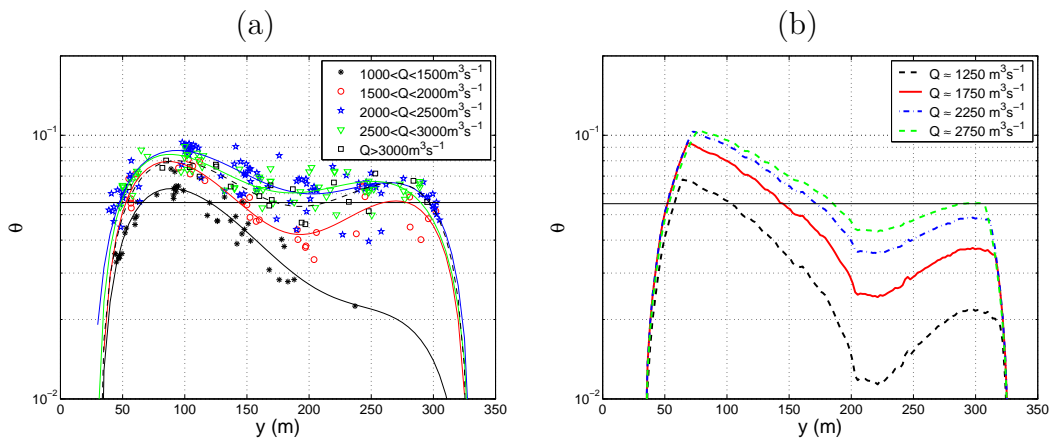critical bed shear stress for the inception of transport.

Fig. 7. Dimensionless bed shear stress distribution in the active channel estimated
from field data (a) and computed for four different water discharges (b) (the hori-
zontal full line corresponds to $\theta_{cr} = 0.055$).

4.3 Distribution of bedload transport over the cross-section

In Fig. 8a, measured values of local bedload transport are presented through-
out the section for the same five different ranges of discharges. The five lines
correspond to a fit of field data for the corresponding five ranges of water dis-
charge. When $Q < 1500 \text{ m}^3 \text{ s}^{-1}$, sediment transport is concentrated on the left
(deeper) part of the main channel. When $Q > 1500 \text{ m}^3 \text{ s}^{-1}$, sediment trans-
port is still prevailing in this part but transport over the bar on the right hand
side of the channel becomes progressively more pronounced as Q increases. It
should be noted that when $Q > 2000 \text{ m}^3 \text{ s}^{-1}$, bedload sediment transport on
the left hand side of the main channel seems to be independent of Q or even
is a decreasing function of Q while the distribution in the active channel is
getting more uniform throughout the whole profile. This is consistent with the

bed shear stress estimated from velocity measurements (*cf.* Fig. 7a), indicating a similar trend between the local bed shear stress in the main channel and the water discharge when $Q > 2500$ m^3 s^{-1}. This may be explained by the location of the main flow, and the velocity maximum, which moves toward the middle part of the section for large water depth.
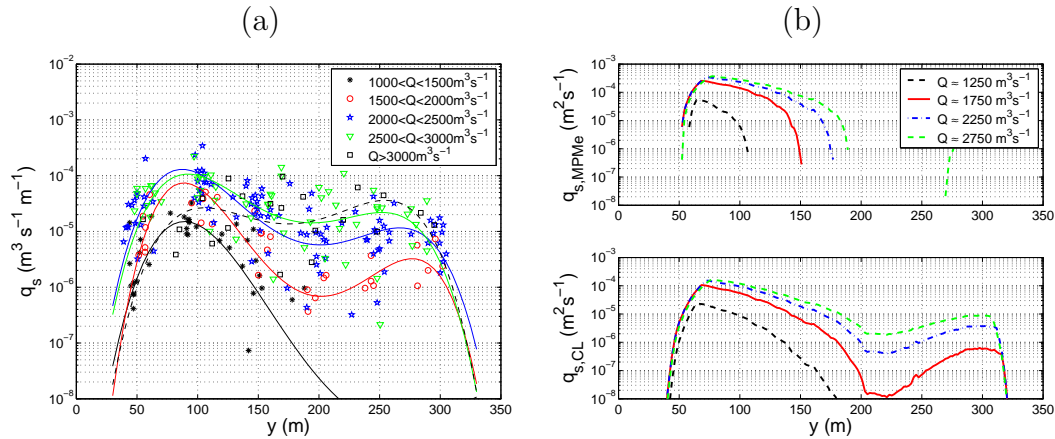

Fig. 8. Bedload transport distribution in the active channel estimated from field data (a) and computed for four different water discharges using either the MPMe formula (b-up) or the CL formula (b-down).

Following the previous results, bedload transport appears to be generally much lower on the right part (over the bar) of the channel where the bed shear stresses are generally lower because of the lower water depth. The ratio of the bedload magnitude over the bar to the bedload magnitude in the deepest part of the channel varies from 1/20 for $1500 < Q < 2000$ m^3 s^{-1}, 1/10 for $2000 < Q < 2500$ m^3 s^{-1}, 1/5 for $2500 < Q < 3000$ m^3 s^{-1}, and 1 when $Q > 3000$ m^3 s^{-1}. For $Q > 3000$ m^3 s^{-1}, transport is becoming higher over the bar due to flow acceleration. This is confirmed by the results from the MPMe and CL formulae (*cf.* Fig. 8b). When $Q > 1500$ m^3 s^{-1}, the two studied formulae suggest a sediment transport prevailing in the deepest part of the main channel but the variations throughout the section are stronger than suggested by field data (*cf.* Fig. 8a). Indeed, because both bedload formulae are functions of the Shields parameter to the power 3/2, the variations in the bed shear stress observed across the section are emphasized. The MPMe formula induces no sediment transport for $y > 200$ m whatever the discharge; and in the deepest part of the main channel ($70 < y < 150$ m), it tends to overestimate the bedload transport. As the CL formula is not as sensitive as the MPMe formula to the critical bed shear stress for the inception of movement, it yields more realistic results compared to field data although underestimated over the bar.

15

4.4 Total bedload transport over the cross-section

From the predicted distribution of the local bedload transport throughout the section using either MPMe or CL formulae (*cf.* Fig. 8b), one can compute the total bedload transport across the section. In Fig. 9, the total bedload discharge rating curves are computed using the MPMe and CL formulae based on the sum of the predicted local values across the section and on the more conventional global value based on cross-sectional average parameters to compute the mean Shields parameter and sediment transport, as it is often done in 1D modelling. Results are plotted together with field data. It should be noted that uncertainties for the experimental data are in the order of a factor 2 or 3 as uncertainty on the bedload rate measured locally should be combined with the uncertainty due to the limited number of measurements throughout the section (spatial integration). As shown by Seed (1996), using mean bed shear stress (section-averaged) to estimate the total bedload transport is clearly not appropriate. For the Danube River, where bed shear stresses are of the same order of magnitude as the critical bed shear stress for inception of transport, large underestimation of the total bedload is obtained using mean values of the bed shear stress. On the other hand, estimating the total sediment transport using a bed shear stress distribution throughout the cross-section yields much better results. In Fig. 9, one can observe that both MPMe and CL formulae underestimate bedload transport for the low water discharges, which confirms the sensitivity to θ_{cr} and to the bed shear stress distribution for low discharges. The MPMe formula tends to overestimate the total bedload transport as it usually overestimates bedload transport in the deepest part of the main channel (where θ is always above θ_{cr} and where most of the bedload transport is observed). It is a direct consequence of the observations made previously (cf. Fig. 4) for local bedload transport. For large water discharges, as the local bed shear stress distribution is getting more and more uniform over the section, the difference between the two methods (direct computation or from the bed shear stress distribution) should get smaller. However, as discussed before, the MP method still predicts significant differences in the bed shear stresses between the main channel and the bar. The nearly constant velocity for $Q > 3000$ m^3 s^{-1} estimated from the fit to field data (see Fig. 6) yields a decreasing mean bed shear stress with Q as the water depth is increasing and $k_s = 2d_{b,90}$ is fixed. As a consequence, the computed total bedload transport is decreasing with Q for $Q > 3000$ m^3 s^{-1}.
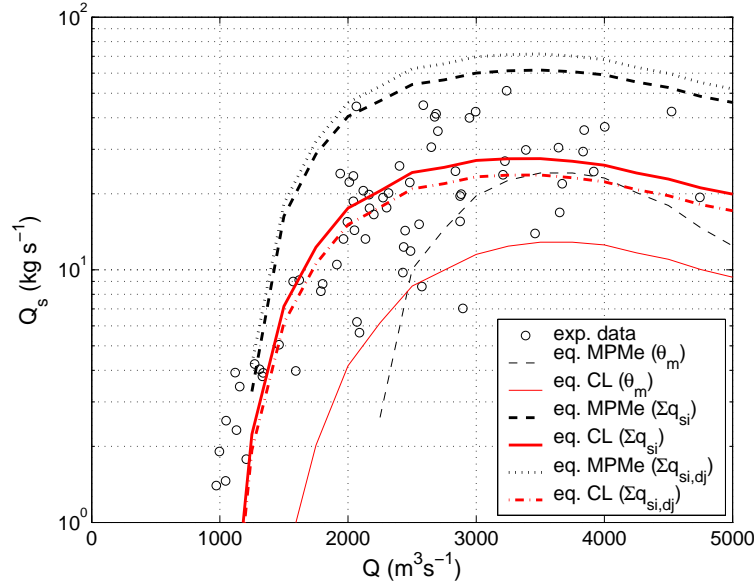
Fig. 9. Total bedload transport over the cross-section as a function of the water discharge using the MPMe and CL formulae with the mean bed shear stress θ_m, and by computing local bed shear stress and bedload transport q_{si} and summing q_{si} over the section using a single grain size d_{50} (Σq_{si}), or by describing the grain size distribution into five classes with a grain size d_j (Eqs. 11 and 8 with $b = b_{WC}$: $\Sigma q_{si,dj}$).

5 Effect of grain size distribution

To take into account the grain size distribution, the total bedload transport has been computed using five different classes for the grain size distribution of the bed material, *i.e.* $d_{b,10} = 5$ mm, $d_{b,30} = 7$ mm, $d_{b,50} = 9$ mm, $d_{b,70} = 15$ mm, and $d_{b,90} = 22$ mm, where each of these classes represents 20% of the bed characteristics. Bedload transport was computed for each class assuming a varying critical bed shear stress for the initiation of motion, $\tau_{cr,j}$, including a hiding factor. This hiding factor includes two main effects of a non-uniform mixture: fine sediments are protected by coarser sediments, and coarser sediments are more exposed and may also move easier because of the presence of fine sediments. Ferguson *et al.* (1989), Parker *et al.* (1990) or Wilcock & Crowe (2003) suggested that in a mixed size gravel bed of average d_{50}, which can be described by n classes with a grain size d_j, the critical bed shear stress for each of these classes, $\tau_{cr,j}$, is not constant (and equal to τ_{cr}) but varies as a function of a hiding factor defined such as,

$$\tau_{cr,j} = \tau_{cr} \left(\frac{d_j}{d_{50}} \right)^b \tag{8}$$

where $0 < b \leq 1$. Ferguson *et al.* (1989) suggested to use $b = b_{Fer} = 0.12$ based on field data. Wilcock & Crowe (2003) found a value that varies from 0.12 if $d_j < d_{50}$ to 0.67 if $d_j > d_{50}$, according to $b = b_{WC} = 0.67/[1+\exp(1.5-d_j/d_{50})]$.

On the other hand, a constant roughness height ($k_s = 2d_{b,90}$) was chosen as the bed shear stress should be the same whatever the sediment size.

The total bedload transport is computed as:

$$q_{s,\Sigma} = \frac{1}{5} \left(q_{s,d10} + q_{s,d30} + q_{s,d50} + q_{s,d70} + q_{s,d90} \right) \tag{9}$$

where the sediment transport corresponding to each class $q_{s,dj}$ is calculated depending on the formula,

$$
\begin{cases}
q_{s,dj} = 8\sqrt{(s-1)gd_j{}^3}(\theta_j - \theta_{cr,j})^{3/2} & \text{(MPMe)} \\[2ex]
q_{s,dj} = 12\sqrt{(s-1)gd_j{}^3}\theta_j{}^{3/2}\exp\left(-4.5\dfrac{\theta_j}{\theta_{cr,j}}\right) & \text{(CL)}
\end{cases}
\tag{10}
$$

with θ_j is the Shields parameters for the class of size d_j, and and $\theta_{cr,j}$ its critical value for the threshold for entrainment. Using Eq. 8, these equations may be rewritten as a function of the Shields parameter based on d_{50} :

$$
\begin{cases}
q_{s,dj} = 8\sqrt{(s-1)gd_{50}{}^3}\left[\theta - \left(\dfrac{d_j}{d_{50}}\right)^b \theta_{cr}\right]^{3/2} & \text{(MPMe)} \\[3ex]
q_{s,dj} = 12\sqrt{(s-1)gd_{50}{}^3}\theta^{3/2}\exp\left[-4.5\left(\dfrac{d_{50}}{d_j}\right)^b \dfrac{\theta}{\theta_{cr}}\right] & \text{(CL)}
\end{cases}
\tag{11}
$$

From Eq. 11, it appears that taking into account grain size distribution affects only the critical bed shear stress in the formulae (Eqs. 3 and 4, respectively). For large bed shear stresses, similar results should be obtained. In this particular study, as the bed shear stress is generally close to its critical value, effects may be not negligible. In Fig. 9, one can see that the calculation of the total bedload transport using five different classes (with $b = b_{WC}$) does not affect significantly the bedload magnitude. However, the two formulae behave differently: using MPMe formula, $\Sigma q_{si} < \Sigma q_{si,dj}$, while using CL formula $\Sigma q_{si} > \Sigma q_{si,dj}$. If the calculation is done with $b = b_{Fer}$, similar results are obtained.

As shown previously, bedload grain size analysis indicates that all sediments from the bed were transported apart the coarsest sediments ($d_{90} < d_{b,90}$). Assuming a description of the bed mixture with 5 classes of equal proportion,

a slight evolution of these proportions is expected for the bedload mixture as coarser sediments are partially transported. Based on field data, the proportion of the 5 classes for the bedload material is estimated in order to obtain $d_{90} = 18$ mm (cf. Tab. 1). However, it should be noted that there is a small bias as the bedload sampler yields an underestimation of the finest particles proportion (smaller than the mesh size, i.e. $d < 0.3$mm) and so yields a small overestimation of d_{90}. This description also affects the proportion of the three finer classes with d_{10}, d_{30}, and d_{50}. If one assumes all fine sediments $d < d_{70}$ are transported, the proportion of these three classes should yet evolve similarly.

For both formulae, bedload grain size analysis is derived from the ratio between the bedload transport rate of one class and the total bedload transport rate. The fine sediment classes tend to dominate the total sediment transport, since no transport (or much lower) is predicted for coarser sediment class. Reminding that d_{50} and d_{90} are slightly overestimated for the bedload material, better results are obtained for the coarser classes using $b = b_{WC}$ than $b = b_{Fer}$. For the CL formula, as it yields positive sediment transport rate even for the coarser class, effects are slightly smaller compared to the MPMe formula.

	Q	d_i (mm)					d_{50}	d_{90}
	(m³/s)	5	7	9	15	22	(mm)	(mm)
bed material (estim.)		20%	20%	20%	20%	20%	9	22
bedload (estim.)		23%	23%	23%	22%	8%	8.2	18
MPMe	1500	29%	25%	15%	17%	14%	7.8	20
$b = b_{Fer}$	3000	26%	24%	15%	19%	16%	8.2	21
MPMe	1500	39%	32%	18%	10%	0%	6.6	13
$b = b_{WC}$	3000	34%	30%	17%	15%	4%	7.0	16
CL	1500	26%	23%	21%	17%	14%	8.1	20
$b = b_{Fer}$	3000	25%	22%	21%	17%	15%	8.2	21
CL	1500	33%	28%	23%	12%	4%	7.2	14
$b = b_{WC}$	3000	31%	27%	23%	13%	5%	7.3	16

Table 1. Estimation of the bedload grain size distribution into the five classes as a function of the bedload formula used and discharge.

6 Conclusion

A comprehensive experimental data set for bedload transport on a large river, the Danube River in Slovakia, is presented. It allows a better understanding of the bed shear stress and bedload transport distribution across a typical section of a large river with a navigation channel, even if some uncertainties

exist because of the unsteadiness of the flow during flood events. For the Danube River, it appeared that the bed shear stresses are very close to and often lower than the estimated critical bed shear stress for the inception of movement whatever the water discharge.

The use of a bed shear stress distribution method appears to be very important to estimate properly the total bedload transport throughout a section. The proposed method, which is a simple geometrical distribution derived from the MP method, improves significantly the results even if it ignores secondary currents, curvature effects or flow acceleration/deceleration. This study confirms the results by Seed (1996): using the mean bed shear stress (even if it is properly estimated), as it is often done in morphodynamic 1D models, is not appropriate for large rivers. It yields severe underestimation, especially for relatively low discharges. As observed by Habersack & Laronne (2001) or Frings & Kleinhans (2008), a high spatial variability of the grain-size distributions would also induce a larger variability in bed shear stresses but also a much larger variability in bedload transport along the cross section. When using a 1D model, the application of bedload formulae on local parameters and so the distribution of the bed shear stress throughout the section appear to be necessary.

It is also essential to properly account for effects of the critical bed shear stress for inception of movement into a bedload formula. Similar observation was done by Habersack & Laronne (2002) using their own field measurements. Formulae using the excess bed shear stress such as the extented Meyer-Peter & Müller (1948) formula yield no transport as soon as $\theta < \theta_{cr}$ even if there are some uncertainties on the prediction of θ_{cr}. Since it corresponds a probabilistic phenomenon, one cannot say that there is no transport even when $\theta < \theta_{cr}$. Moreover, when θ is slightly larger than θ_{cr}, models based on the excess bed shear stress (MPMe-type formulae) tend to overestimate the bedload transport. A formula based on a statistical approach (CL-type formulae) for the inception of transport such as suggested by Einstein (1950) should be less sensitive to the uncertainty on the estimation of θ_{cr}.

When applying these formulae to a sediment mixture with 5 classes, both formulae yield similar results for the overall bedload transport magnitude compared to the estimation based on the d_{50} only. However, they tend to overestimate bedload for the finer classes. The bedload grain size distribution appeared to be relatively poorly predicted. Equations suggested by Ferguson *et al.* (1989) or Wilcock & Crowe (2003) for the interaction between different classes of sediments still need to be validated and improved for an application

20

in the field. For a morphodynamic 1D model, because of the large uncertainties in the estimation of the local bed shear stress and critical bed shear stress, the multiclass procedure to compute bedload transport and its grain-size distribution is not straightforward to use and evaluate.

Acknowledgment

References

Abdel-Fattah, S., Amin, A., Van Rijn, L., 2004. Sand transport in Nile River, Egypt. J. Hydraulic Eng. 130 (6), 488–500.

Ackers, P., White, W. R., 1973. Sediment transport: New approach and analysis. J. Hydraulic Division 99 (11), 2041–2061.

Allen, J., 1985. Principles of physical sedimentology. George Allen & Unwin Ldt, London, UK.

Buffington, J., Montgomery, D., 1997. A systematic analysis of eight decades of incipient motion studies, with special reference to gravel-bedded rivers. Water Resources Res. 33 (8), 1993–2029.

Bunte, K., Ab, S., Potyondy, J., Ryan, S., 2004. Measurement of coarse gravel and cobble transport using portable bedload traps. J. Hydraulic Eng. 130 (9), 879–893.

Camenen, B., Bayram, A., Larson, M., 2006. Equivalent roughness height for plane bed under steady flow. J. Hydraulic Eng. 132 (11), 1146–1158.

Camenen, B., Larson, M., 2005. A bedload sediment transport formula for the nearshore. Estuarine, Coastal & Shelf Science 63, 249–260.

Cardoso, A., Graf, W., Gust., G., 1989. Uniform flow in a smooth open channel. J. Hydraulic Res. 27 (5), 603–616.

Ehrenberger, R., 1931. Direct bedload measurements on the Danube at Vienna, and their results to date [Direkte geschiebemessungen an der Donau bei Wien und deren bisherige ergebnisse]. Die Wasserwirtschaft 34, 1–19, (In German).

Einstein, H., 1950. The bed-load function for sediment transportation in open channel flows. Tech. Rep. 1026, U.S. Dept. of Agriculture, Techn. Bulletin, Washington D.C., USA.

Ferguson, R., Prestegaard, K., Ashworth, P., 1989. Influence of sand on hydraulics and gravel transport in a braided gravel bed river. Water Resources Res. 25 (4), 635–643.

Frings, R., Kleinhans, M., 2008. Complex variations in sediment transport at three large river bifurcations during discharge waves in the river Rhine. Sedimentology 55, 1145–1171.

Gaweesh, M., Van Rijn, L., 1994. Bed-load sampling in sand-bed rivers. J. Hydraulic Eng. 120 (12), 1364–1384.

Graf, W., 1971. Hydraulics of Sediment Transport. McGraw-Hill, New York, USA.

Habersack, H., Laronne, J., 2001. Bed load texture in an alpine gravel bed river. Water Resources Res. 37 (12), 33593370.

Habersack, H., Laronne, J., 2002. Evaluation and improvement of bed load discharge formulas based on Helley-Smith sampling in an alpine gravel bed river. J. Hydraulic Eng. 128 (5), 484–499.

Habersack, H., Seitz, H., Laronne, J., 2008. Spatio-temporal variability of bedload transport rate: analysis and 2d modelling. Geodinamica Acta 21 (1-2), 67–79.

Hey, R., 1979. Determinate hydraulic geometry of river channels. J. Hydraulic Division 104, 869–885.

Holubová, K., Capeková, Z., Szolgay, J., 2004. Impact of hydropower schemes at bedload regime and channel morphology of the Danube River. In: Greco, M., Carravetta, A., Della Morte, R. (Eds.), River Flow, Proc. 2nd Int. Conf. on Fluvial Hydraulics. June 2004, Napoli, Italy, pp. 135–141.

ISO 748, 2007. Hydrometry: Measurement of liquid flow in open channels using current-meters or floats. Tech. rep., International Organization for Standardization, 58 p.

Kamphuis, J., 1974. Determination of sand roughness for fixed beds. J. Hydraulic Res. 12 (2), 193–203.

Khodashenas, S., Paquier, A., 1999. A geometrical method for computing the distribution of boundary shear stress across irregular straight open channels. J. Hydraulic Res. 37 (3), 381–388.

Leopold, L., Emmett, W., 1976. Bedload measurements, East Fork River, Wyoming. Proc. Nat. Acad. Sci., USA 73 (4), 1000–1004.

McLean, D., Church, M., Tassone, B., 1999. Sediment transport along lower Fraser River: 1. measurements and hydraulic computations. Water Resources Res. 35 (8), 2533–2548.

Meyer-Peter, E., Müller, R., 1948. Formulas for bed-load transport. In: IInd IAHR Congress. Stockholm, Sweden, pp. 39–64.

Parker, G., 1990. Surface-based bedload transport relation for gravel rivers. J.

Hydraulic Res. 28 (4), 417–436.

Recking, A., Frey, P., Paquier, A., Belleudy, P., Champagne, J., 2008. Feedback between bed load transport and flow resistance in gravel and cobble bed rivers. Water Resources Res. 44, 21 p.

Seed, D., March 1996. Lateral variation of sediment transport in rivers. SR 454, HR Walligford, Wallingford, UK.

Shields, A., 1936. Anwendung der Ahnlichkeits-mechanik und der turbulenzforschung auf die geshiebebewegung [application of similarity principles and turbulence research to bed-load movement]. Preussische Versuchsanstalt fur Wasserbau und Schiffbau 26, berlin.

Shiono, K., Knight, D., 1991. Turbulent open channel flows with variable depth across channel. J. Fluid Mechanics 222, 617–646.

Smart, G., Maurice, M., Walsh, J., 2002. Relatively rough flow resistance equations. J. Hydraulic Eng. 128 (6), 568–578.

Soulsby, R., 1997. Dynamics of marine sands, a manual for practical applications. Thomas Telford, London, UK, ISBN 0-7277-2584 X.

Sumer, B., Kozakievicz, A., Fredsœ, J., Deigaard, R., 1996. Velocity and concentration profiles in the sheet-flow layer of movable bed. J. Hydraulic Eng. 122 (10), 549–558.

Thomas, W., Prashum, A., 1977. Mathematical model of scour and deposition. J. Hydraulic Division 110, 16131641.

Wilcock, P., Crowe, J., 2003. Surface-based transport model for mixed-size sediment. J. Hydraulic Eng. 129 (2), 120–128.

Wong, M., Parker, G., 2006. Reanalysis and correction of bed-load relation of meyer-peter and mller using their own database. J. Hydraulic Eng. 132 (11), 1159–1168.

Yalin, M., 1977. Mechanics of Sediment Transport. Pergamon Press, Oxford, 2nd edition.

Yang, S., Lim, S., 1997. Mechanism of energy transportation and turbulent flow. J. Hydraulic Eng. 123 (8), 684–692.